AIAA Atmospheric Flight Mechanics Conference and Exhibit
20 - 23 August 2007, Hilton Head, South Carolina

AIAA 2007-6630

CrossMark
click for updates

Roll Coupling Effects on the Stability Margins for VEGA Launcher

Christophe R. Roux [1] and Irene Cruciani[2]
ELV, Colleferro, Italy, 00034

We present a new method applied in the VEGA launcher development to quantify the effect of roll coupling on the stability margins. First we show in time domain simulations the instability due to roll rate, not visible in stability analysis of an axial symmetric launcher when only considering a plan model (either in yaw or in pitch channel). Linear models from Phillips theory for aircrafts and from Lazennec for launchers demonstrate to be inadequate to give stability conditions for VEGA and its control laws. Hence a more complete model is introduced, which shows the roll coupling effect on the attitude stability. The roll coupled linear model allows computing the maximum roll rate acceptable before instability. For roll rate values under this limit, we express the impact of roll rate in terms of reduction of stability gain margin, firstly in a SISO approach classical for rocket control and then in a more general MIMO background. Finally we describe techniques used to recover part of the lost margins, showing their benefits and their drawbacks.

Downloaded by INST TEC DE AERONAUTICA (ITA) on January 23, 2017 | http://arc.aiaa.org | DOI: 10.2514/6.2007-6630

Nomenclature

a	=	lift force coefficient
A_6	=	aerodynamic instability coefficient
β_ψ, β_θ	=	thrust deflection along yaw and pitch axes
$\beta^{Gyro}{}_\psi$, $\beta^{Gyro}{}_\theta$	=	additional command for gyroscopic compensation
$C_{N\alpha}$	=	aerodynamic normal gradient coefficient
$\Delta\psi$, $\Delta\theta$	=	pitch and yaw angle errors
Δ_{11}, Δ_{12},Δ_{21}, Δ_{22}	=	elements of the disturbance matrix
$\Delta\beta_\psi$, $\Delta\beta_\theta$	=	elements of the disturbance matrix in yaw and pitch
F	=	inertia ratio factor
γ	=	longitudinal acceleration
γ_T	=	longitudinal acceleration due to thrust
Ixx, Iyy, Izz	=	principal moments of inertia
$\hat{I}xx, \hat{I}yy, \hat{I}zz$	=	on-board scheduled principal moments of inertia
K_1	=	controllability coefficient
$\hat{K}_1$	=	on-board scheduled controllability coefficient
k_ψ, k_θ	=	proportional gains on yaw and pitch errors
$k_{\psi D}$, $k_{\theta D}$	=	derivative gains on yaw and pitch errors
k_Y, k_Z	=	gains on side and normal errors
k_{YD}, k_{ZD}	=	gains on side and normal velocity errors
λ	=	factor for gyroscopic compensation
L, M, N	=	external moments in body axes
M_ψ, M_q	=	yaw moments' derivatives
N_θ, N_r	=	pitch moments' derivatives
p, q, r	=	components of angular rate in body axes

[1] Control Engineer, GNC Department, ELV Spa, 00034 Colleferro (Roma), Italy, christophe.roux@elv.it, and AIAA Member.
[2] Control Engineer, GNC Department, ELV Spa, 00034 Colleferro (Roma), and PhD Student at University La Sapienza (Roma), Italy, irene.cruciani@elv.it.

Copyright © 2007 by ELV S.p.A. Published by the American Institute of Aeronautics and Astronautics, Inc., with permission.

$\hat{p}, \hat{q}, \hat{r}$	=	estimated angular rate
ρ	=	air density
S_{ref}	=	reference surface
V	=	module of the air relative velocity
ω_{yaw}, ω_{pitch}	=	yaw and pitch frequency in closed loop
ω_{ψ}, ω_{θ}	=	yaw and pitch normalized frequency in closed loop
ω_P	=	frequency in closed loop
x_{CoG}	=	centre of gravity abscissa
x_{CP}	=	centre of pressure abscissa
x_T	=	thrust application point abscissa
Y, Z	=	lateral drift
ζ_{ψ}, ζ_{θ}	=	pitch and yaw damping factor in closed loop
ζ_P	=	damping factor in closed loop

Downloaded by INST TEC DE AERONAUTICA (ITA) on January 23, 2017 | http://arc.aiaa.org | DOI: 10.2514/6.2007-6630

I. Introduction

FOR engineers involved in missile control, roll rate is often created to increase missile stability. On the other hand, for launcher scientists, the roll rate is generally controlled to zero or nearly zero. In this case the assumption of two uncoupled axes of pitch and yaw remains valid and engineers can keep on designing two separate Thrust Vector Control (TVC) laws, identical in case of axial-symmetric launcher.

In presence of roll, the axes of pitch and yaw become coupled. If the roll is not controlled to zero but only constrained to remain below a limit value (which is less demanding for a dedicated roll control system), the question hence arises to analyze the effect of this coupling on the stability and margins of the control law. Actually, the scope is to keep valid the decoupled control laws design and just to quantify or at least to minimize the impact of roll rate on the architecture of the control law.

After presenting the context of the VEGA launcher in Section II, we show in Section III the time domain simulations which show the instability due to roll coupling. In Section IV we propose a comparison between roll coupled linear models: the Phillips' model applied to slender aircrafts[1], the Lazennec's model[9] applied to an axial-symmetric launcher, and our model, which takes into account both the attitude and the transversal component of the control law, and allows defining stability conditions with respect to roll rate evidencing the phenomenon of roll coupling resonance.

In Section V we use the model to evaluate the impact of roll rate on the Single Input Single Output (SISO) stability margins, then in Section VI we present a Multi Input Multi Output (MIMO) approach to the margin evaluation more general than the SISO approach. Finally, in Section VII, we describe the techniques that have been applied to recover part of the lost margins.

II. Context

VEGA is the new European Small Launch Vehicle developed under the responsibility of ESA, European Space Agency. The prime contractor for the launch vehicle is ELV, a Joint Venture between Avio S.p.A and Italian Space Agency (ASI). Avio S.p.A is also the prime contractor of the P80 Solid Rocket Motor (SRM) under the Centre National d'Etudes Spatiales (CNES) contract, on behalf of ESA. The P80 development is suited to meet two specific objectives, to serve as first stage of VEGA, and to prepare the technologies for a future improvement of the Ariane 5 boosters.

The VEGA in-orbit capability is 1500 Kg payload at 700 Km altitude circular Polar Earth Orbit (PEO) as reference mission, with a launch performed from the Centre Spatial Guyanais (CSG) in Kourou, the European Space Center.

The propulsion system of VEGA is composed of three solid propellant motors providing thrust for the lower 1st, 2nd, and 3rd stages, namely P80, Zefiro 23 and Zefiro 9, and a bi-propellant liquid engine for transfer orbit injection, scattering compensation and final orbit injection (AVUM).

All four stages are controlled via thrust vectoring system. The fourth stage also includes a Roll and Attitude Control System (RACS).

The RACS is dedicated to control attitude during ballistic phases and is also in charge of the roll rate control during propelled phases. Limit the roll means that the roll rate is not actually controlled to zero but constrained to

remain below a threshold value. This value should result of a trade off between the robustness of the control laws to roll rate and the control authority of the RACS.

Thus the question is to select a limit roll rate. On one hand, we make a budget for the roll rate which could be encountered by considering the different sources of torque:

- propulsive and aerodynamic torques in presence of offset of the centre of gravity and/or the thrust application point,
- disturbing torque observed on solid propellant motors[3],
- aerodynamic roll torque due to protrusions caused by raceways tunnels.

On the other hand, the impact of roll rate is analyzed on the TVC control stability.

The TVC control is initially designed to fulfill SISO requirements (expressed in terms of classical gains and phase margins) based on a perfect separation of the yaw and pitch channels. A new calculation of stability margins needs thus to be performed.

The new margins are still computed in a SISO frame whereas the system actually is a MIMO system. In any case, the objective is to keep the very classical notions used in rocket control of low frequency gain margin, phase margin, and high frequency gain margin as usually read on Nichols plot. As a complement a MIMO approach is then proposed.

Downloaded by INST TEC DE AERONAUTICA (ITA) on January 23, 2017 | http://arc.aiaa.org | DOI: 10.2514/6.2007-6630

III. Simulations

The effect of the roll rate coupling is investigated by performing 6 Degrees of Freedom (6DoF) time domain simulations with the simulator developed in ELV.

This simulator implements a nonlinear 6DoF launcher model including elastic and sloshing modes, actuators and sensors models as well as GNC algorithms.

The TVC controller consists of a feedback of two measurements: attitude angles provided by an Inertial Reference Frame and drift velocity with respect to the programmed trajectory, which is provided by open-loop guidance.

Due to the axial-symmetry of the body, the control laws are identical for both axes and the two channels are assumed to be uncoupled. This assumption does not remain valid in presence of roll rate.

A roll rate limit above which the launcher becomes instable is clearly observed and the limit value is shown to be strongly dependant of the mission and launcher characteristics (i.e. trajectory, geometry, payload, thrust and associated dispersions).

Figure 1 shows attitude error angles (yaw error $\Delta\psi$ and pitch error $\Delta\theta$) for three values of roll rate: 0, 60 and 120°/s. In case of a roll rate of 135°/s, not presented on the figure, the launcher is unstable.

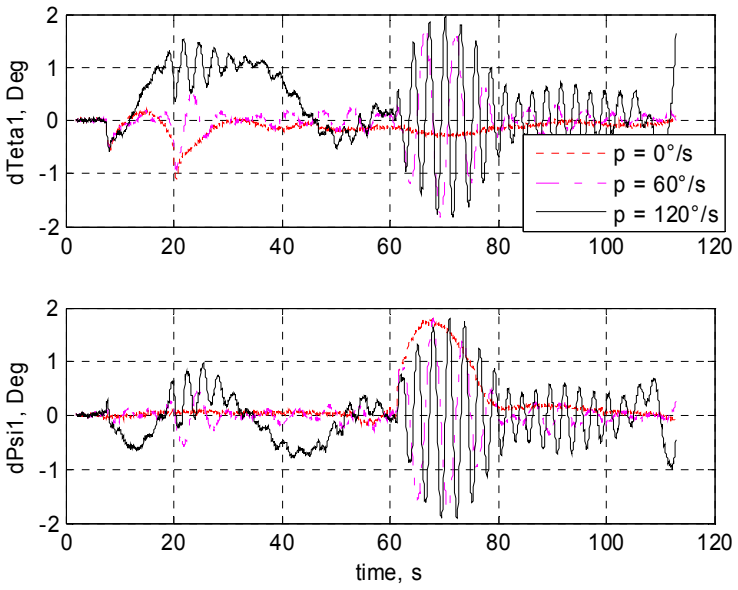

Figure 1. Attitude Errors $\Delta\theta$, $\Delta\psi$ for p = 0, 60 and 120°/s

This leads us to theoretically explain the observed behavior by a linear model, presented in the next section. Thanks to this model, we verify not only the stability of the launcher, but also calculate stability margins in presence of roll coupling.

IV. Linear Time Invariant Model

The models used for stability analysis and design control are classically linear time-invariant (LTI) models: they result of a linearization around a reference trajectory and are time-invariant by assuming the parameters (trajectory and propulsive parameters, geometrical and mass characteristics) are frozen at each flight time. Note that the linearization is possible, since in atmospheric flight angle of attack is limited by structural constraints to small values.

For control studies the degrees of freedom are the attitude error angles (yaw $\Delta\psi$ and pitch $\Delta\theta$) and the lateral drift (Z or Y). The equations of rigid motion consist of:

- a kinematical equation relating attitude angles and angular velocity,
- moments equation driving the attitude angles evolution (Euler equations including gyroscopic torque),
- lateral forces equation driving the drift velocity evolution.

For an axial-symmetric body (identical lateral moments of inertia) the first Euler equation becomes:

$$Iyy = Izz \quad \Rightarrow \quad Ixx \cdot \dot{p} = L \qquad (1)$$

We assume that at first order the roll motion is decoupled from pitch and yaw dynamics and roll rate can be considered as an external input. In the frame of a frozen parameters analysis we can then suppose the roll rate as a constant or a slowly varying term. Instead the Euler equations in pitch and yaw are roll coupled.

Kinematical equations and force equations are also coupled by the roll rate as shown in the complete system:

$$\begin{aligned} \Delta\dot{\psi} &= q + p \cdot \Delta\theta \\ \Delta\dot{\theta} &= r - p \cdot \Delta\psi \end{aligned} \qquad (2)$$

$$\begin{aligned} \dot{q} &= A_6 \cdot (\Delta\psi + \frac{\dot{Z}}{V}) + \left(1 - \frac{Ixx}{Iyy}\right) \cdot p \cdot r + K_1 \cdot \beta_\psi \\ \dot{r} &= A_6 \cdot (\Delta\theta - \frac{\dot{Y}}{V}) - \left(1 - \frac{Ixx}{Iyy}\right) \cdot p \cdot q + K_1 \cdot \beta_\theta \end{aligned} \qquad (3)$$

$$\begin{aligned} \ddot{Z} &= -a \cdot (\Delta\psi + \frac{\dot{Z}}{V}) - p \cdot \dot{Y} - \gamma \cdot \Delta\psi - \gamma_T \cdot \beta_\psi \\ \ddot{Y} &= a \cdot (\Delta\theta - \frac{\dot{Y}}{V}) + p \cdot \dot{Z} + \gamma \cdot \Delta\theta + \gamma_T \cdot \beta_\theta \end{aligned} \qquad (4)$$

where:

$Ixx << Iyy$ for a slender body

$A_6 = \frac{1}{2}\rho V^2 S_{ref} \frac{C_{N\alpha}\left(x_{CP} - x_{CoG}\right)}{Iyy} > 0$, for aerodynamic unstable rockets

$a = \frac{1}{2}\rho V^2 S_{ref} \frac{C_{N\alpha}}{mass}$

$\gamma = \frac{Thrust - Drag}{mass}$

Downloaded by INST TEC DE AERONAUTICA (ITA) on January 23, 2017 | http://arc.aiaa.org | DOI: 10.2514/6.2007-6630

$$\gamma_T = \frac{Thrust}{mass}$$

$$K_1 = \frac{Thrust\left(x_T - x_{CoG}\right)}{Iyy} < 0$$

and where we have used for the attack angles projected on both channels the following expressions:

$$\alpha_\psi = \Delta\psi + \frac{\dot{Z}}{V} \quad (5)$$

$$\alpha_\theta = \Delta\theta - \frac{\dot{Y}}{V} \quad (6)$$

The complete model we have developed also includes bending and sloshing modes, tail wags dog effect as well as actuator and sensor dynamics and the TVC digital controller. Note that also bending modes and sloshing modes are coupled via roll rate[8].

The digital controller mainly consists of a feedback in rigid state vector and a set of filters to cope with the bending modes. We report below the simplified equation for the TVC controller.

$$\begin{cases} \beta_\psi = k_\psi \Delta\psi + k_{\psi D}\Delta\dot{\psi} + k_Z Z + k_{ZD}\dot{Z} \\ \beta_\theta = k_\theta \Delta\theta + k_{\theta D}\Delta\dot{\theta} + k_Y Y + k_{YD}\dot{Y} \end{cases} \quad (7)$$

with:

$$k_\psi = k_\theta$$
$$k_{\psi D} = k_{\theta D}$$
$$k_Z = -k_Y$$
$$k_{ZD} = -k_{YD}$$

A useful parallel to understand the instability can be drawn from rotational dynamics of slender aircrafts. In case we neglect the translational motion, the system of equations Eqs (2), (3) and (7) is a special case of the model introduced by Phillips[1, 2]. In its model the external moments are proportional to attitude error and angular velocity, since only due to aerodynamic moments:

$$M = M_\psi \cdot \Delta\psi + M_q \cdot q$$
$$N = N_\theta \cdot \Delta\theta + N_r \cdot r$$

Hence we obtain:

$$\begin{aligned} \dot{q} - \frac{Izz - Ixx}{Iyy}\cdot p \cdot r - \Delta\psi \cdot \frac{M_\psi}{Iyy} - q \cdot \frac{M_q}{Iyy} = 0 \\ \dot{r} + \frac{Iyy - Ixx}{Izz}\cdot p \cdot q - \Delta\theta \cdot \frac{N_\theta}{Izz} - r \cdot \frac{N_r}{Izz} = 0 \end{aligned} \quad (8)$$

and, introducing the normalized frequency as ratio between the frequency of the non rolling aircraft to the steady rolling frequency p and the damping ratio:

$$\omega_\psi = \frac{1}{p}\cdot\sqrt{-\frac{M_\psi}{Iyy}} = \frac{1}{p}\cdot\omega_{yaw}, \quad 2\cdot\zeta_\psi\cdot\omega_\psi = \frac{1}{p}\cdot\left(-\frac{M_q}{Iyy}\right)$$

Downloaded by INST TEC DE AERONAUTICA (ITA) on January 23, 2017 | http://arc.aiaa.org | DOI: 10.2514/6.2007-6630

$$\omega_\theta = \frac{1}{p}\cdot\sqrt{-\frac{N_\theta}{Izz}} = \frac{1}{p}\cdot\omega_{pitch}, \quad 2\cdot\zeta_\theta\cdot\omega_\theta = \frac{1}{p}\cdot\left(-\frac{N_r}{Izz}\right)$$

we can write the equations of the slender aircraft:

$$\begin{bmatrix}\ddot{\psi}\\ \ddot{\theta}\end{bmatrix} + p\cdot\begin{bmatrix} 2\cdot\zeta_\psi\cdot\omega_\psi & -\left(1+\frac{Izz-Ixx}{Iyy}\right)\\ \left(1+\frac{Iyy-Ixx}{Izz}\right) & 2\cdot\zeta_\theta\cdot\omega_\theta\end{bmatrix}\begin{bmatrix}\dot{\psi}\\ \dot{\theta}\end{bmatrix} + p^2\cdot\begin{bmatrix}\omega_\psi^2-\frac{Izz-Ixx}{Iyy} & -2\cdot\zeta_\psi\cdot\omega_\psi\\ 2\cdot\zeta_\theta\cdot\omega_\theta & \omega_\theta^2-\frac{Iyy-Ixx}{Izz}\end{bmatrix}\begin{bmatrix}\psi\\ \theta\end{bmatrix} = \begin{bmatrix}0\\0\end{bmatrix} \quad (9)$$

Neglecting damping effect and considering a plan mass distribution ($Izz = Ixx+Iyy$) we obtain:

$$\begin{bmatrix}\ddot{\psi}\\ \ddot{\theta}\end{bmatrix} + p\cdot\begin{bmatrix}0 & -2\\ 1+F & 0\end{bmatrix}\begin{bmatrix}\dot{\psi}\\ \dot{\theta}\end{bmatrix} + p^2\cdot\begin{bmatrix}\omega_\psi^2-1 & 0\\ 0 & \omega_\theta^2-F\end{bmatrix}\begin{bmatrix}\psi\\ \theta\end{bmatrix} = \begin{bmatrix}0\\0\end{bmatrix} \quad (10)$$

having used:

$$F = \frac{Iyy-Ixx}{Izz}$$

Stability conditions for slender aircrafts can be stated as:

$$\left(\omega_\psi^2-1\right)\left(\omega_\theta^2-F\right)>0 \quad \Rightarrow \quad \begin{cases} p<\omega_{yaw} \\ p<\dfrac{\omega_{pitch}}{\sqrt{F}}\end{cases} \cup \begin{cases} p>\omega_{yaw} \\ p>\dfrac{\omega_{pitch}}{\sqrt{F}}\end{cases} \quad (11)$$

which can be associated to a resonance between rolling frequency and yawing (or pitching) frequency.

The obtained conditions (11) give zones of instability in the plane of the pitch and yaw frequencies (ω_{pitch}, ω_{yaw}) by varying roll rate for different inertial configurations. For a given aircraft, corresponding to a ratio ($\omega_{pitch}/\omega_{yaw}$) and represented by a line in the Phillips' diagram (Fig.2, line A, B or C), we found two points (e.g. p_{A1} and p_{A2}) intersecting the boundaries of the divergence region: they correspond to two different roll rate values between which the aircraft is unstable.

With this simplified model the launcher is actually never unstable when varying roll rate because the body is axial-symmetric: the pitch and yaw dynamics in closed loop are identical ($\omega_{pitch} = \omega_{yaw}$) and the system never enters the divergence region, as shown in Fig. 2, line B.

For an axial - symmetrical body ($Iyy = Izz$, $\omega_\psi = \omega_\theta$, $\zeta_\psi = \zeta_\theta$), the system becomes:

$$\begin{bmatrix}\ddot{\psi}\\ \ddot{\theta}\end{bmatrix} + p\cdot\begin{bmatrix} 2\cdot\zeta_\psi\cdot\omega_\psi & -\left(2-\frac{Ixx}{Iyy}\right)\\ \left(2-\frac{Ixx}{Iyy}\right) & 2\cdot\zeta_\psi\cdot\omega_\psi\end{bmatrix}\begin{bmatrix}\dot{\psi}\\ \dot{\theta}\end{bmatrix} + p^2\cdot\begin{bmatrix}\omega_\psi^2-\left(1-\frac{Ixx}{Iyy}\right) & -2\cdot\zeta_\psi\cdot\omega_\psi\\ 2\cdot\zeta_\psi\cdot\omega_\psi & \omega_\psi^2-\left(1-\frac{Ixx}{Iyy}\right)\end{bmatrix}\begin{bmatrix}\psi\\ \theta\end{bmatrix} = \begin{bmatrix}0\\0\end{bmatrix} \quad (12)$$

which is a linear mechanical system, whose stability conditions in absence of damping are:

$$\omega_\psi^2-\left(1-\frac{Ixx}{Iyy}\right)+\frac{1}{4}\left(2-\frac{Ixx}{Iyy}\right)^2>0 \quad \Rightarrow \quad \omega_\psi^2 = \frac{1}{p^2}\left(\frac{-M_\psi}{Iyy}\right) > -\frac{1}{4}\left(\frac{Ixx}{Iyy}\right)^2 \quad (13)$$

Downloaded by INST TEC DE AERONAUTICA (ITA) on January 23, 2017 | http://arc.aiaa.org | DOI: 10.2514/6.2007-6630

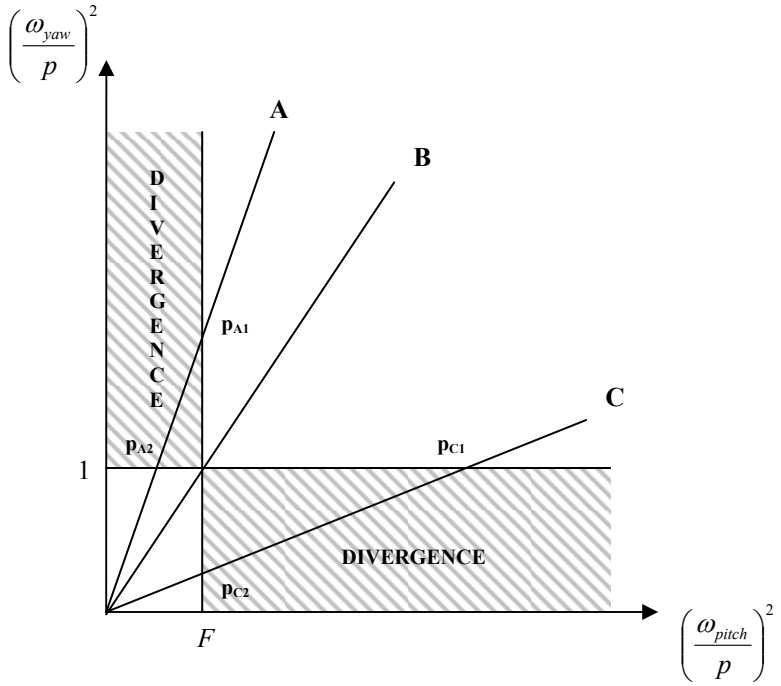

Figure 2. Philips diagram for stability

If $\omega_\psi^2 > 0$ the condition is always true, while for $\omega_\psi^2 < 0$ ($M_\psi > 0$), we obtain the stability condition for projectiles and spinned missiles:

$$S = \frac{1}{4}\frac{p^2}{\left(M_\psi / Iyy\right)}\left(\frac{Ixx}{Iyy}\right)^2 > 1 \quad (14)$$

Lazennec[9] introduces in its linear model of an axial-symmetric launcher the control feedback, showing stability conditions in two different cases:

- feedback in ($\Delta\psi$,$\Delta\theta$) for the attitude error, (q, r) for the angular rate;
- feedback in ($\Delta\psi$,$\Delta\theta$) for the attitude error, ($\Delta\dot{\psi}$, $\Delta\dot{\theta}$) for the angular rate;

$$\frac{M}{Iyy} = \begin{cases} K_1 \cdot \left(k_\psi \cdot \Delta\psi + k_{\psi D} \cdot q\right) & case\ a \\ K_1 \cdot \left(k_\psi \cdot \Delta\psi + k_{\psi D} \cdot \Delta\dot{\psi}\right) & case\ b \end{cases}$$

$$\frac{N}{Iyy} = \begin{cases} K_1 \cdot \left(k_\psi \cdot \Delta\theta + k_{\psi D} \cdot r\right) & case\ a \\ K_1 \cdot \left(k_\psi \cdot \Delta\theta + k_{\psi D} \cdot \Delta\dot{\theta}\right) & case\ b \end{cases}$$

Hence Euler's equations become:

$$\begin{cases} \dot{q} = p \cdot \left(1 - \frac{Ixx}{Iyy}\right) \cdot r + \left(A_6 + K_1 \cdot k_\psi\right) \cdot \Delta\psi + \left(K_1 \cdot k_{\psi D}\right) \cdot \left(q + \nu \cdot p \cdot \Delta\theta\right) \\ \dot{r} = -p \cdot \left(1 - \frac{Ixx}{Iyy}\right) \cdot q + \left(A_6 + K_1 \cdot k_\psi\right) \cdot \Delta\theta + \left(K_1 \cdot k_{\psi D}\right) \cdot \left(r - \nu \cdot p \cdot \Delta\psi\right) \end{cases} \quad (15)$$

Downloaded by INST TEC DE AERONAUTICA (ITA) on January 23, 2017 | http://arc.aiaa.org | DOI: 10.2514/6.2007-6630

with ν = 0 for case *a* and ν = 1 for case *b*. Introducing the closed loop frequency and damping, defined as:

$$\omega_P = \sqrt{-\left(A_6 + K_1 \cdot k_\psi\right)}, \quad 2 \cdot \zeta_P \cdot \omega_P = -K_1 \cdot k_{\psi D}$$

the system becomes:

$$\begin{bmatrix} \Delta\dot{\psi} \\ \dot{q} \\ \Delta\dot{\theta} \\ \dot{r} \end{bmatrix} = \begin{bmatrix} 0 & 1 & p & 0 \\ -\omega_P^2 & -2 \cdot \zeta_P \cdot \omega_P & -2 \cdot \nu \cdot p \cdot \zeta_P \cdot \omega_P & \left(1 - \frac{Ixx}{Iyy}\right) \cdot p \\ -p & 0 & 0 & 1 \\ 2 \cdot \nu \cdot p \cdot \zeta_P \cdot \omega_P & -\left(1 - \frac{Ixx}{Iyy}\right) \cdot p & -\omega_P^2 & -2 \cdot \zeta_P \cdot \omega_P \end{bmatrix} \cdot \begin{bmatrix} \Delta\psi \\ q \\ \Delta\theta \\ r \end{bmatrix} \quad (16)$$

We can compute stability conditions using Routh criterion, applied to its fourth order polynomial equation:

$$p(s) = s^4 + \left(4 \cdot \zeta_P \cdot \omega_P\right) \cdot s^3 + \left(2 \cdot \omega_P^2 + p^2 \cdot \left(1 - \frac{Ixx}{Iyy}\right)^2 + p^2 + 4 \cdot \zeta_P^2 \cdot \omega_P^2\right) \cdot s^2 +$$

$$\ldots + \left(-4 \cdot \zeta_P \cdot \omega_P \left(\nu \cdot p^2 \cdot \left(1 - \frac{Ixx}{Iyy}\right) - \omega_P^2 + p^2 \cdot (\nu - 1)\right)\right) \cdot s + \left(\left(2 \cdot p \cdot \omega_P \cdot (1 - \nu)\right)^2 \cdot \zeta_P^2 + \left(\omega_P^2 - p^2 \cdot \left(1 - \frac{Ixx}{Iyy}\right)\right)^2\right)$$

Stability Conditions for a 4th order polynomial $p(s) = s^4 + a_1 s^3 + a_2 s^2 + a_3 s + a_4$ are:

$$\begin{cases} a_1 > 0, \quad a_2 > 0, \quad a_4 > 0 \\ \Delta_3 = a_1\left(a_2 a_3 - a_1 a_4\right) - a_3^2 > 0 \end{cases}$$

The first three conditions are true for each value of roll rate p. The only active condition is:

$$\Delta_3 = -16 \cdot \zeta_P^2 \cdot \omega_P^2 \cdot \left(\left(p + \left(1 - \frac{Ixx}{Iyy}\right) \cdot p\right)^2 + 4 \cdot \zeta_P^2 \cdot \omega_P^2\right) \cdot \left(\nu \cdot p^2 \cdot \left(\nu - \frac{Ixx}{Iyy}\right) - \omega_P^2\right) > 0$$

$$\Rightarrow \quad \nu \cdot p^2 \cdot \left(\nu - \frac{Ixx}{Iyy}\right) - \omega_P^2 < 0$$

For case *a* (ν = 0) stability is assured for each value of p, while for case *b* (ν = 1) the stability condition is a typical resonance condition:

$$p^2 < \omega_P^2 \cdot \left(1 - \frac{Ixx}{Iyy}\right)^{-1} \quad (17)$$

The two different roll coupling effects on stability are shown in Fig. 3, where are presented the poles (real part, module and opposite damping) versus roll rate in the two cases *a* and *b*. Case *a* is always stable, while for case *b* the occurrence of instability is visible above 130°/s, where the damping of one pole becomes negative. The resonance is visible on the modulus graph, when one of the mode linearly decreases down to the 0 rd/s axis for roll rate close to 130°/s: in the system of equations reduced to rotational motion, this mode is simply $|p - \omega_P|$.

From this analysis we can derive that an appropriate feedback on the attitude rate (the angular velocity instead of the attitude error rate) can overcome the instability due to roll coupling effects. Nevertheless, Lazennec's model doesn't take into account lateral feedback, which is necessary to avoid a lateral deviation of the launcher from the reference trajectory.

Using this further feedback component, and introducing translational motion (Eq.(4)), we obtain a system of order 8, whose stability conditions are not simple to be expressed analytically (for example by Routh criterion), but can be deduced from a numerical computation of the eigenvalues.

Downloaded by INST TEC DE AERONAUTICA (ITA) on January 23, 2017 | http://arc.aiaa.org | DOI: 10.2514/6.2007-6630

As can be seen from Fig.4, the lateral feedback changes completely our conclusions: case *a* is dramatically impacted by roll coupling (instability is visible since 30°/s), while case *b* is practically unchanged. The choice of the feedback on the derivation of attitude error instead of angular velocity is therefore the one to be applied.

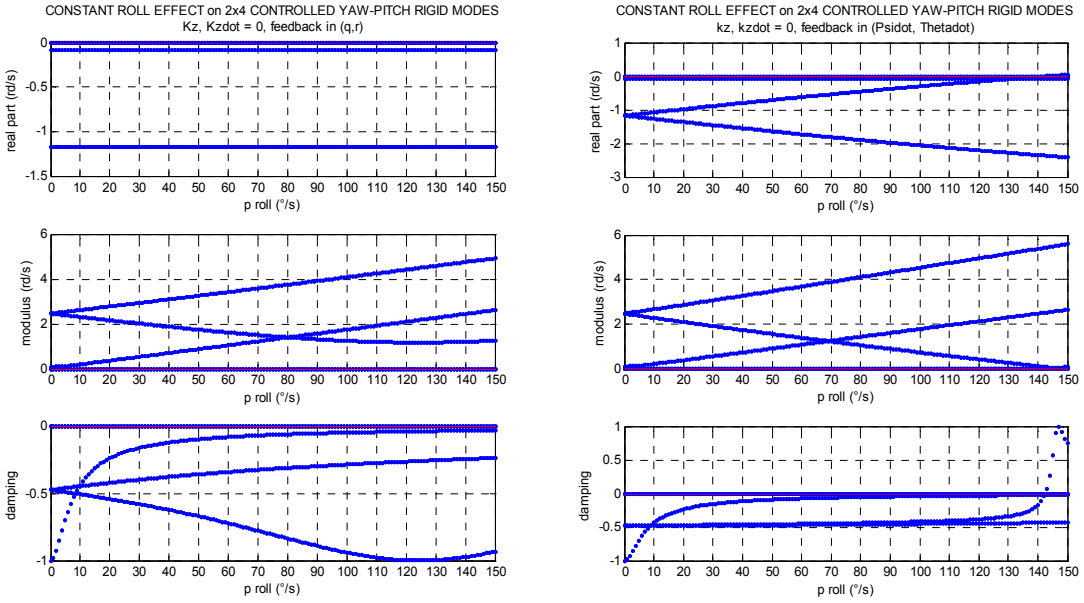

a) **b)**

Figure 3. Poles vs p for feedback in (q, r) and feedback in ($\dot{\psi}, \dot{\theta}$) for cases a) and b)

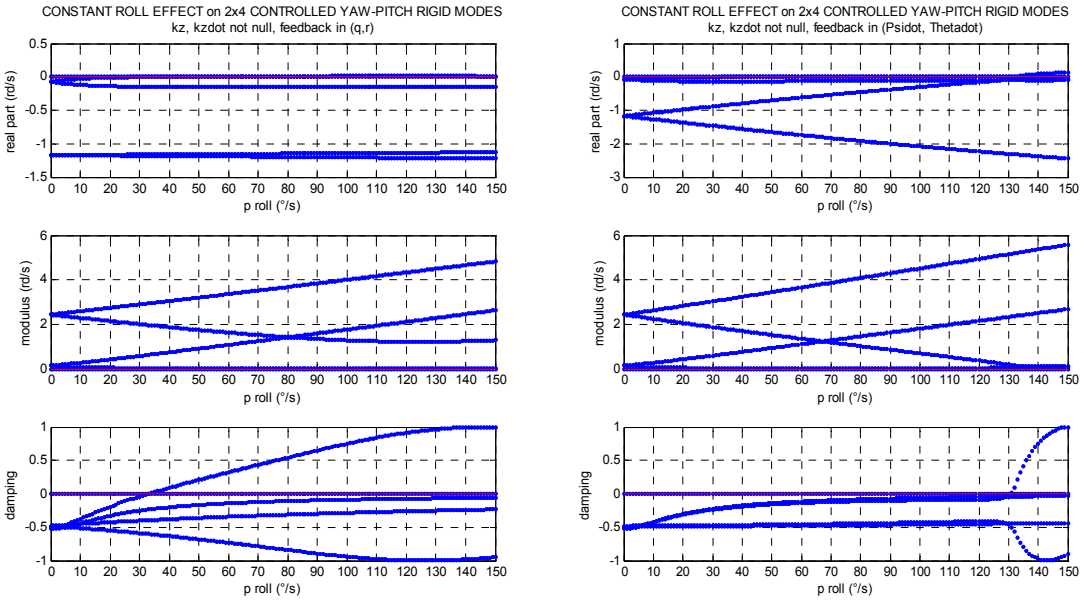

a) **b)**

Figure 4. Poles vs p for feedback in (q, r) and feedback in ($\dot{\psi}, \dot{\theta}$), with lateral feedback, for cases a) and b)

Downloaded by INST TEC DE AERONAUTICA (ITA) on January 23, 2017 | http://arc.aiaa.org | DOI: 10.2514/6.2007-6630

Hence the limit roll value is a function of the tuning of the TVC controller and of the launcher characteristics; in particular it increases with the controllability ratio K_1 / A_6 and with the gain on attitude and decreases with the lateral gain, which is responsible of the coupling between angular and transversal equations. Since the launcher characteristics and consequently the tuning of the controller vary during the flight, we can compute a profile of roll rate limit versus time as illustrated in Fig. 5:

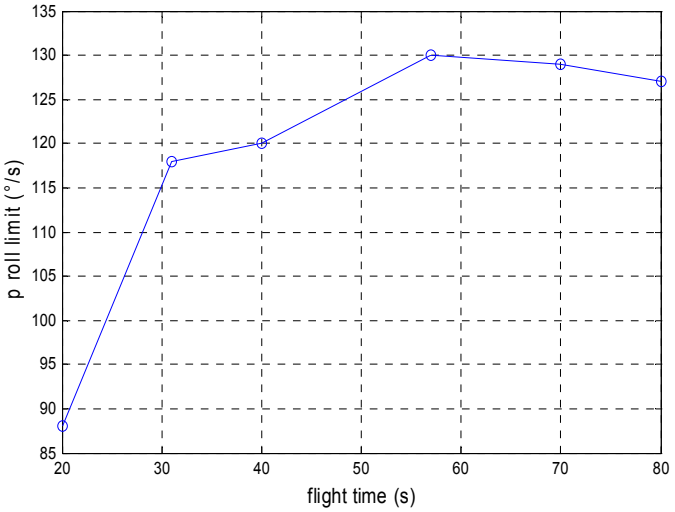

Figure 5. Limit of stability vs Flight Time

V. Loss of SISO Margins

For SISO control of unstable rocket, the stability margins are usually presented as:

- Low Frequency (LF) gain margin (margin of gain reduction), magnitude of the transfer function of the controlled system in open loop at the crossing of the vertical axis at -180 deg above 0dB. This margin appear in case of a vehicle unstable in open-loop;
- phase margin for rigid mode (expressed as delay margin by considering the frequency at which it occurs), phase of the transfer function at the crossing of 0dB axis;
- High Frequency (HF) gain margin (margin of gain increase), magnitude of the transfer function at the crossing of the vertical axis at -180 deg below 0dB;
- margins linked to bending modes (phase margin for phase controlled modes and gain margin for gain controlled modes).

The analysis is made for a given control law designed in a SISO frame and made robust by taking into account a set of nominal and dispersed configurations of the launcher: for a given flight time we consider not only the nominal values but a range of thrust, aerodynamic coefficients, dynamic pressure, inertial and geometric data. The control law is checked to be robust for this set of configurations at null roll rate and fulfills frequency domain requirements.

Starting from this result, we make the SISO analysis of the coupled system (Eqs. (2), (3), (4) and (7)) by imposing different levels of roll rate. For one channel (e.g. yaw) we compute the classical margins putting the other channel (e.g. pitch) in closed loop.

Figure 6 displays three Nichols plots computed with the complete coupled model for three values of the roll rate (0, 60 and 100°/s). We observe that the roll rate decreases the LF margin and that at 100°/s the system is still stable but close to the instability limit at 130°/s. We also notice that the other margins (phase margin and HF gain margin) are influenced too.

Downloaded by INST TEC DE AERONAUTICA (ITA) on January 23, 2017 | http://arc.aiaa.org | DOI: 10.2514/6.2007-6630

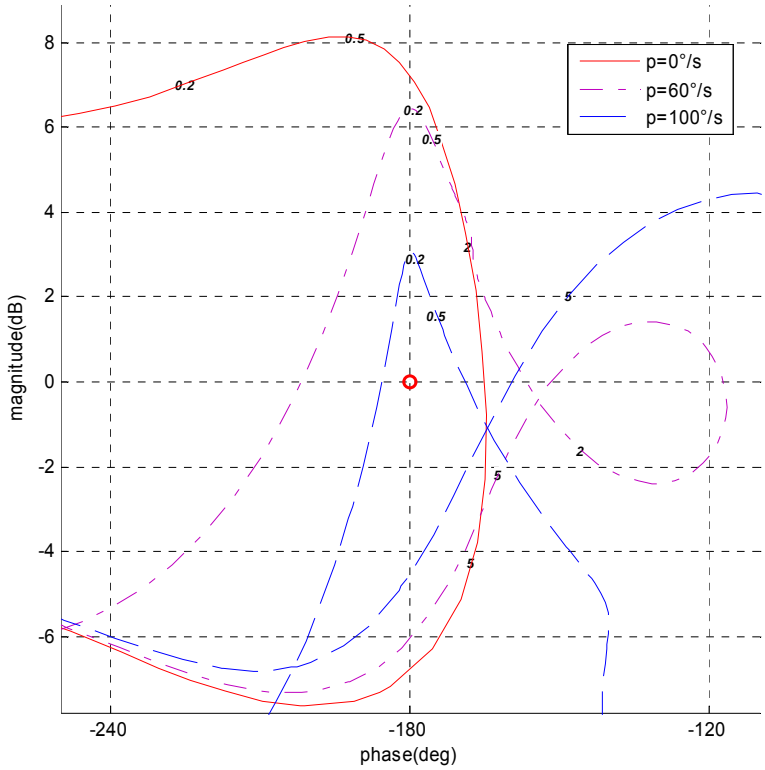

Figure 6. Nichols plot of the complete coupled model for roll rate = 0, 60 and 100 °/s

VI. Definition of MIMO Gain Margins

The drawback of the coupled SISO approach is that only one control loop is disturbed at the same time. Hence we are not sure that the margins exactly reflect the robustness of the system.

MIMO systems require the use of the general framework of MIMO analysis (e.g. structured singular values) and several generalizations of the notions of gain and phase margins have been proposed[6,7].

Nevertheless the considered system is actually not a full MIMO, because is almost diagonal except for the roll coupling terms. It is more exactly a coupling of two basically SISO systems, the coupling increasing with roll rate. Consequently, the classical SISO approach is not incorrect but needs a refinement.

For this reason we change the scalar perturbation with a matrix of perturbations Δ, which affects both yaw and pitch channels. The MIMO scheme to be considered consists of a loop including:

- the launcher dynamics (rigid states plus elastic modes, sloshing modes, actuator and sensor dynamics),
- the GNC gains and filters,
- a disturbance matrix impacting both channels.

The situation can be summarized on the diagram in Fig. 7

The perturbation matrix has two fundamental properties which simplify the problem:

1. the coupling is only due to roll rate, hence the perturbation matrix is diagonal ($\Delta_{12} = \Delta_{21} = 0$);
2. possible uncertainties on the model (as thrust, aerodynamic, actuators' delay) have the same effect on the two channels ($\Delta_{11} = \Delta_{22}$).

Firstly we consider the hypothesis: $\Delta_{12} = \Delta_{21} = 0$ ($\Delta_{11} = \Delta\beta_\psi$, $\Delta_{22} = \Delta\beta_\theta$).

Downloaded by INST TEC DE AERONAUTICA (ITA) on January 23, 2017 | http://arc.aiaa.org | DOI: 10.2514/6.2007-6630

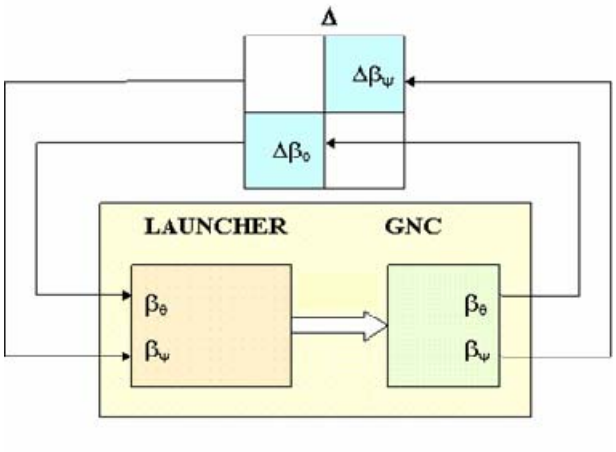

Figure 7. Structure of the disturbed system

Stability analysis can be performed for each level of roll rate by computing the eigenvalues of the closed-loop system varying the disturbing factors ($\Delta\beta_\psi$, $\Delta\beta_\theta$) and by determining the boundary that divides the plan between a stable domain and an unstable domain.

Since there are two parameters to be considered, we can represent the stability domain in the plan ($\Delta\beta_\psi$,$\Delta\beta_\theta$), or, equivalently in dB, in the plan (κ_ψ, κ_θ), where:

$$\kappa_\psi = -20\log_{10}(\Delta\beta_\psi)$$
$$\kappa_\theta = -20\log_{10}(\Delta\beta_\theta)$$

Due to the symmetry between yaw and pitch, the boundary is symmetric with respect to the angle bisector.

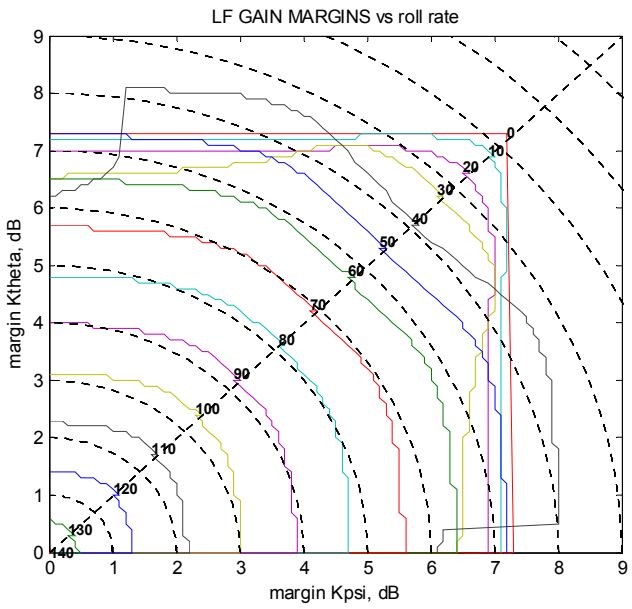

Figure 8. Stability domain computed in MIMO approach at different roll rates (perturbations in dB)

Downloaded by INST TEC DE AERONAUTICA (ITA) on January 23, 2017 | http://arc.aiaa.org | DOI: 10.2514/6.2007-6630

Figure 8 shows such a diagram plotted for different roll rates (0, 10, 20 …, 120° /s). When reasoning in MIMO approach, we have a curve of margins in the plan (κ_ψ, κ_θ). For null roll rate the two channels are decoupled, hence the curve is a square: the margin is the same obtained in absence of roll coupling. For a roll rate different from zero the curve becomes a circle line, because the two channels are no more decoupled. The points on the horizontal (κ_ψ,0) and the vertical (0,κ_θ) axes simply correspond to the SISO margins computed in Section V, because they correspond to the margins computed perturbing only one channel, while the other is closed with no disturb (unitary gain).

Let we consider now the additional property on the perturbation matrix: $\Delta_{11} = \Delta_{22}$. Angle bisector points have the property that they represent a set of perturbations that affect equally both channels, such as thrust dispersion that impacts the controllability coefficient K_1. These margins are the more conservative on the whole set of curves: introducing the norm

$$N_\infty = \min\left[\max\left(\kappa_\psi, \kappa_\theta\right)\right]$$

we found exactly the points on the bisector. For instance at 60°/s the value of N_∞ is less than 5dB on the bisector (MIMO approach), while is 6.5dB on one of the two axes $\kappa_\psi = 0$ or $\kappa_\theta = 0$ (SISO approach).

Figure 9 represents the LF margin in function of roll rate obtained using the points on the angle bisector: comparing it with the LF margin computed in SISO approach (dashed line) it shows that SISO approximation is not appropriate because it overestimates the stability margin, considering the minimum perturbation on a single channel before instability.

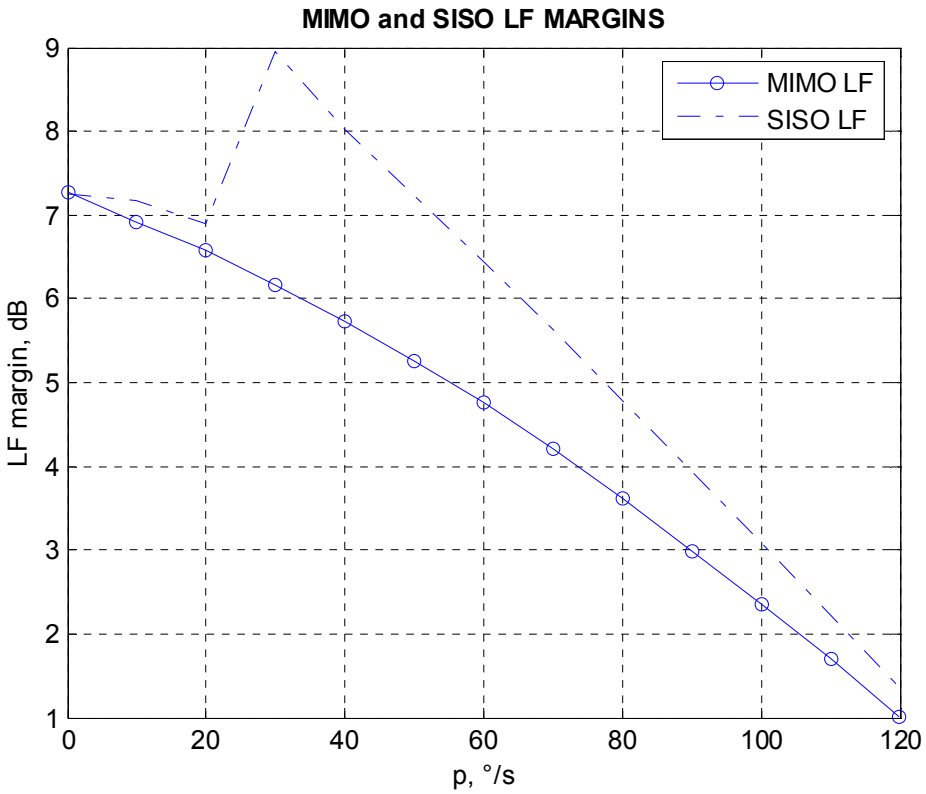

Figure 9. MIMO and SISO LF margins at different roll rates (margins in dB)

Same method can be applied for the computation of gain margin HF and phase margin. In the first case the perturbation matrix will be the identity matrix multiplied by a real gain greater than 1 ($\Delta > 1$), in the second case it will be the identity matrix multiplied by an imaginary negative gain (a delay).

Downloaded by INST TEC DE AERONAUTICA (ITA) on January 23, 2017 | http://arc.aiaa.org | DOI: 10.2514/6.2007-6630

Hereafter in Fig.10 we report plots for MIMO and SISO margins obtained function of roll rate p, between 0 and 120°/s.

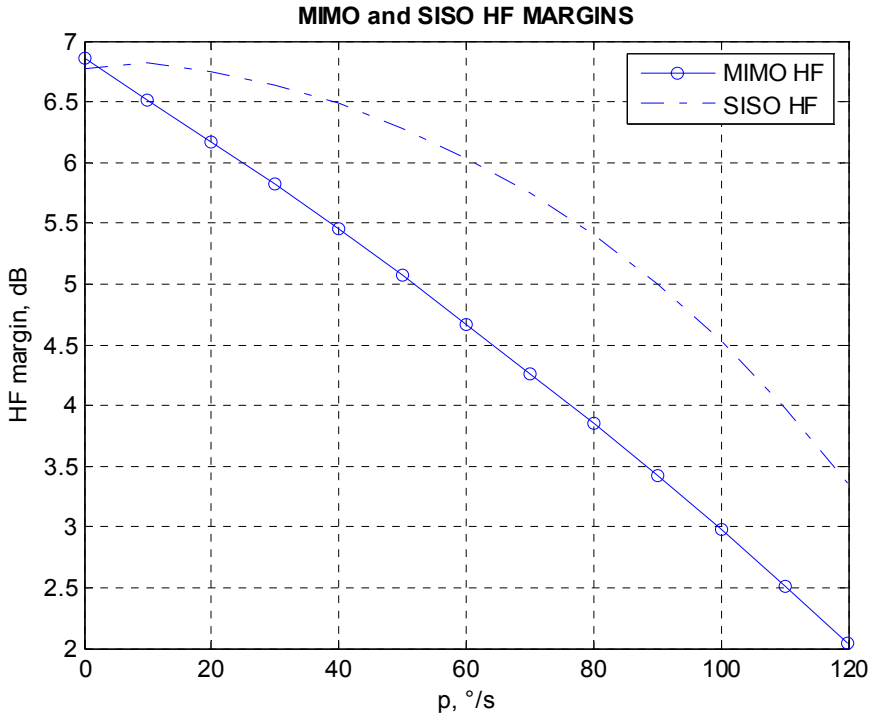

a)

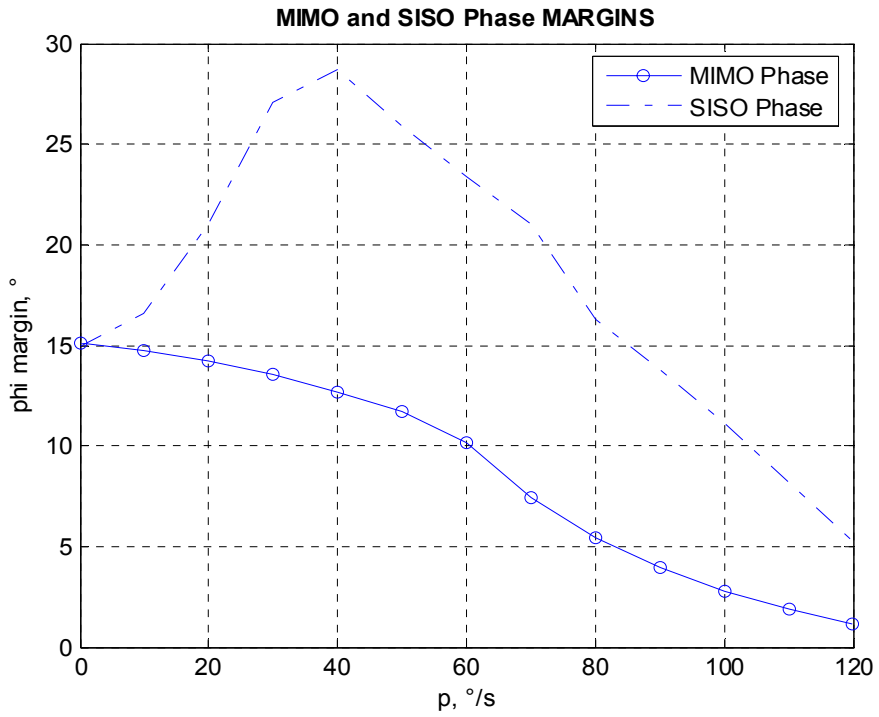

b)

Figure 10. MIMO, SISO HF Margin (a) and MIMO, SISO Phase Margin (b) vs roll rate

Downloaded by INST TEC DE AERONAUTICA (ITA) on January 23, 2017 | http://arc.aiaa.org | DOI: 10.2514/6.2007-6630

VII. Techniques to Recover Margins

To recover part of the lost margins possible solutions are presented hereafter.

A. Gyroscopic compensation

A simple way to recover part of the margins is to perform a compensation of the gyroscopic torque in the moments' equations trying to eliminate the terms in Eq. (3).

$$\beta_{\psi}^{Gyro} = -\frac{\lambda}{\hat{K}_1}\cdot\left(1-\frac{\hat{I}xx}{\hat{I}yy}\right)\cdot\hat{p}\cdot\hat{r}$$
$$\beta_{\theta}^{Gyro} = +\frac{\lambda}{\hat{K}_1}\cdot\left(1-\frac{\hat{I}xx}{\hat{I}yy}\right)\cdot\hat{p}\cdot\hat{q} \qquad (18)$$

Note that even an ideal compensation does not suppress the roll rate coupling since it also appears in the kinematical and in the translational motion equations. Practically this compensation is not perfect since:

- estimated angular rate is based on the formula governing quaternion dynamics and via a filtered derivative of the estimated quaternion and hence $[\hat{p},\hat{q},\hat{r}]\neq[p,q,r]$,
- $\hat{K}_1, \hat{I}xx, \hat{I}yy$ are predicted values of the real parameters,
- λ can be chosen different from 1.

In Fig. 11 we show MIMO LF gain margin (a), HF gain margin (b) and phase margin (c) versus roll rate, in case of: $\lambda = 0$ (no compensation), $\lambda = 0.25$, 0.50, 0.75 and 1, with $\hat{K}_1 = K_1, \hat{I}xx = Ixx, \hat{I}yy = Iyy$.

For what concerns the LF margin, full compensation ($\lambda = 1$) gives an evident benefit: for p = 120°/s the margin goes from 1dB to more than 4.5dB. This is in line with the fact that this margin reflects the stability of the low frequency dynamics (in particular rotational dynamic); hence, having modified Euler's equation through the gyroscopic factor, the benefit on the angular motion is evident.

For what concerns the other margins, the higher frequency dynamics (actuators, filters, sensors…) make the effect of the compensation term less predictable and not always positive. In Fig. 11.b, we notice that the best improvement on HF margin is given for $\lambda = 0.5$ or 0.75, while for $\lambda = 1$ the improvement practically disappears. The effect on the phase margin seems to be less important (Fig. 11.c), but however it isn't always positive.

B. Feedback on translational motion

We said above that the instability appears when the feedback on translational motion is introduced, because it creates a strong coupling between rotational and translational dynamics. Hence a simple way to recover margin, in particular LF margin, is to limit lateral gains, accepting a weaker control of lateral motion. It has to be noticed, however, that a certain level of coupling between rotational and translational motion still exists also for a null value of k_Z and k_{ZD} through aerodynamic moments' expression (in particular attack angle, Eqs. (5)-(6)). In addition, lateral feedback can be minimized but cannot be zero: it allows limiting attack angle and controlling lateral drift of the launcher loosing the nominal direction of the trajectory and having a strong impact on performances.

Finally the optimal value of lateral gains results of a trade off between the need to limit drift and the robustness to a certain level of roll rate.

It is interesting to note that a source of drift motion may be the thrust misalignment. In presence of roll, its effect is partially compensated since averaged.

In Fig. 12 we show the behavior of MIMO margins (LF, HF and phase) varying k_Z and k_{ZD}. Minimum values for k_Z and k_{ZD} assure the highest LF and HF gain margins, but are penalizing in terms of phase margin.

Downloaded by INST TEC DE AERONAUTICA (ITA) on January 23, 2017 | http://arc.aiaa.org | DOI: 10.2514/6.2007-6630

Downloaded by INST TEC DE AERONAUTICA (ITA) on January 23, 2017 | http://arc.aiaa.org | DOI: 10.2514/6.2007-6630

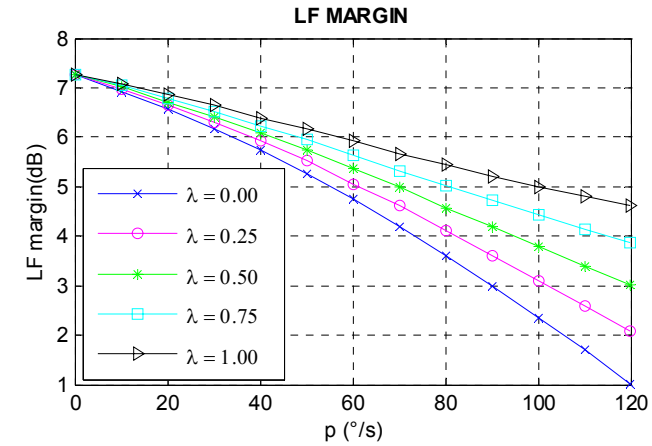

(a)

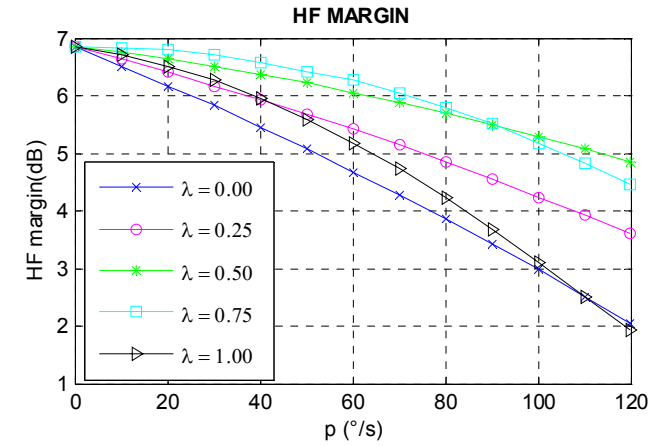

(b)

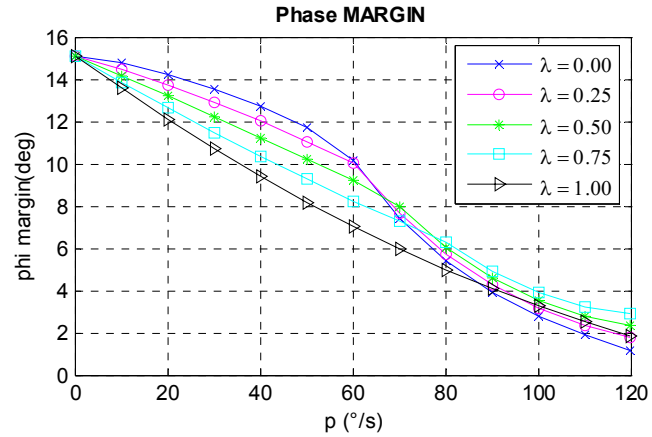

(c)

Figure 11. Gyroscopic Compensation Effect on MIMO LF Margin (a), HF Margin (b) and Phase Margin (c) versus roll rate

Downloaded by INST TEC DE AERONAUTICA (ITA) on January 23, 2017 | http://arc.aiaa.org | DOI: 10.2514/6.2007-6630

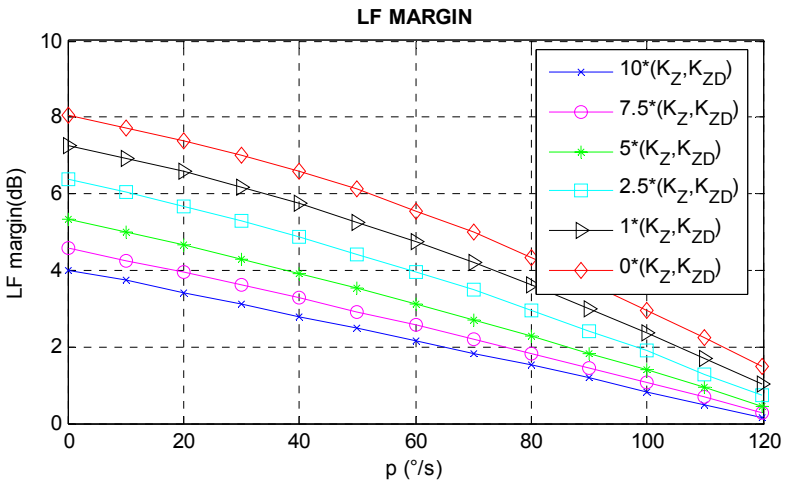

(a)

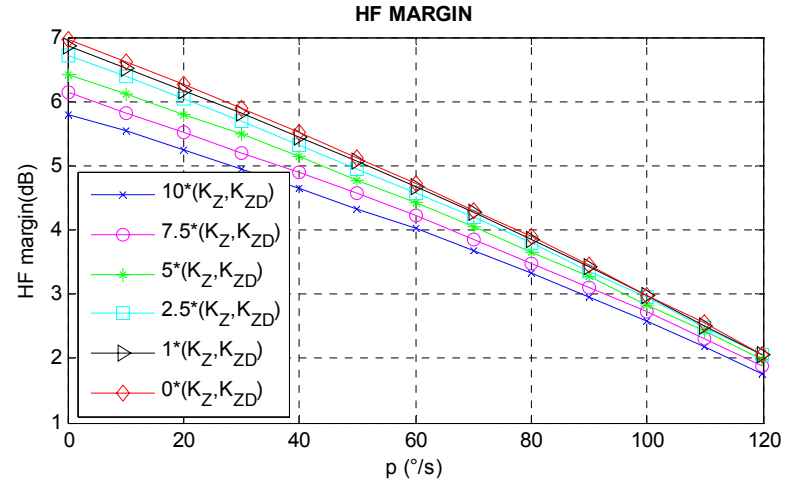

(b)

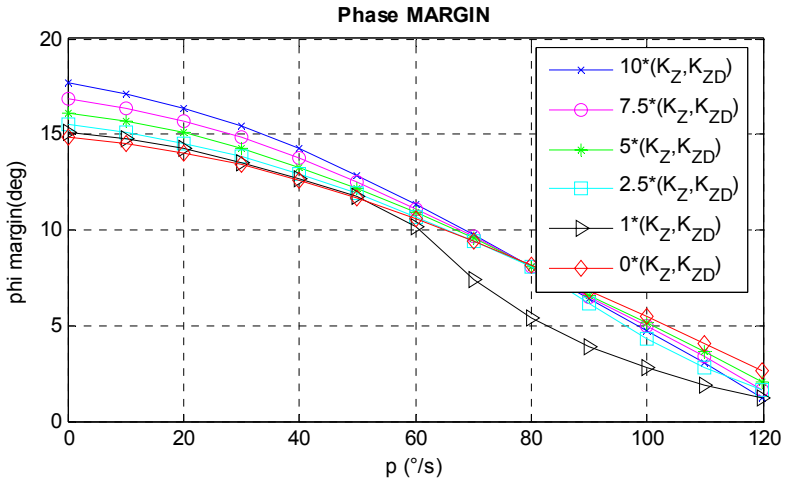

(c)

Figure 12. Lateral Gains Effect on MIMO LF Margin (a), HF Margin (b) and Phase Margin (c) versus roll rate

VIII. Conclusion

Roll coupling effects on stability have been studied on several models (aircrafts, missiles, launchers). For aerodynamic unstable missiles and projectiles, gyroscopic stability condition is achieved for roll rate greater than a value depending on geometrical and aerodynamic characteristics. For slender aircrafts with static stability, roll coupling can induce dynamic instability when roll rate lies inside an interval, function of the ratio between pitch and yaw natural frequencies. For aerodynamic unstable launchers, dynamically stabilized by a classical control law with feedback in angular and lateral motion, instability occurs over a limit roll rate near the closed loop frequency.

The impact of roll coupling on stability has been quantified in terms of loss of margins. The reduction of margins due to the roll rate has been verified in time domain simulations and confirmed by frequency domain analysis.

A MIMO extension of the SISO classical approach has been proposed to take into account disturbances affecting both yaw and pitch channels simultaneously.

This work allows keeping valid the SISO control laws design by means of slight modifications:

- gyroscopic compensation,
- reduction of the translational motion control,
- introduction of the margin reduction due to roll in the stability margins budget.

It allows not controlling roll rate to zero but just limiting it under an optimized value, with a substantial save of RACS propellant mass.

Downloaded by INST TEC DE AERONAUTICA (ITA) on January 23, 2017 | http://arc.aiaa.org | DOI: 10.2514/6.2007-6630

Acknowledgments

We thank Paolo Bini (responsible of the GNC Department in ELV - Colleferro), Piero D. Resta (from ESA/IPT - Frascati) and Benjamin Carpentier (from CNES - Evry) for useful discussions and advices.

References

[1] Philips W,.H, "Effect of Steady Rolling on Longitudinal and Directional Stability", *NASA TN 1627*, June 1948.

[2] Day, R.E., "Coupling Dynamic in Aircraft: a historical perspective", *NASA Special Publication,* 532, 1997.

[3] Knauber, R.N., "Roll Torques Produced by Fixed Nozzle Solid Rocket Motors", *AIAA 95-2874, Conference San Diego*, July 10-12, 1995.

[4] Blakelock, J.H., *Automatic Control of Aircraft and Missiles*, John Wiley and Sons, 1991.

[5] Greensite, A.L, *Analysis and Design of Space Vehicle Flight Control Systems*, Spartan Books, New York, 1970.

[6] Wie, B., *Space Vehicle Dynamics and Control*, AIAA Education Series, 1998.

[7] Mangiacasale, L., *Airplane Control Systems*, Levrotto-Bella, Torino, 1996.

[8] Platus, D.H., "Aeroelastic Stability of Slender Spinning Missile", *Journal of Guidance, Control and Dynamics*, Vol. 15 No. 1, 1992 (144-151).

[9] Lazennec, H., *Pilotage des Missiles et des Véhicules Spatiaux*, Dunod, Paris, 1966.

[10] Jahnke, C., C., "On the roll-coupling instabilities of high-performance aircraft", *Phil. Trans. R. Soc. Lond.* A (1998) 356, pp. 2223-2239.

[11] Charters, A., C., "The Linearized Equations of Motion underlying the Dynamic Stability of Aircraft, Spinning Projectiles and Symmetrical Missiles", *NASA Technical Note 3350,* 1955.

[12] Naik, S., D., "A Note on Stability of Motion of a Projectile", *Sadhana*, Vol. 26, Part 4, August 2001, pp.379-385.